Electronic supplementary information for:

Coexistence of 1:1 and 2:1 inclusion complexes of indigo carmine

Oksana Yanshyna,[a] Liat Avram,[b] Linda J. W. Shimon,[b] and Rafal Klajn*[a]

[a]Department of Organic Chemistry, Weizmann Institute of Science, Rehovot 76100, Israel
[b]Department of Chemical Research Support, Weizmann Institute of Science, Rehovot 76100, Israel

Table of contents

1. Materials and methods

Cage **1** was synthesized according to a previously reported literature procedure.[2] Indigo carmine **2** (disodium salt; dye content >80%) was purchased from Fischer Chemical (product number I16625) and purified by reverse-phase flash chromatography on a Biotage Isolera One instrument equipped with a BUCHI FlashPure Cartridge (product number 145152103). 100 mg of **2** was dissolved in 2 mL of water and applied onto the column; impurities were removed by gradient elution with MeCN→8:2 *v*/*v* MeCN/water, and the residue was dissolved in water; see Fig. S1 for the NMR spectrum of purified **2**). NMR spectra were recorded on a Bruker Avance III 400 MHz spectrometer or a Bruker Avance III HD 500 MHz spectrometer. All the spectra were recorded in D_2O at room temperature; chemical shifts (δ) are given in ppm relative to residual proton solvent resonance (4.79 ppm). UV–Vis absorption spectra were recorded with an Agilent Cary 60 spectrophotometer. Emission spectra were recorded with a Shimadzu spectrofluorophotometer RF-5301 PC. For details on the X-ray data collection and refinement, see Section 5. Isothermal calorimetry titration (ITC) experiments were performed on a MicroCal PEAQ-ITC instrument under ambient conditions (T = 25 ºC); for further details, see Section 6.

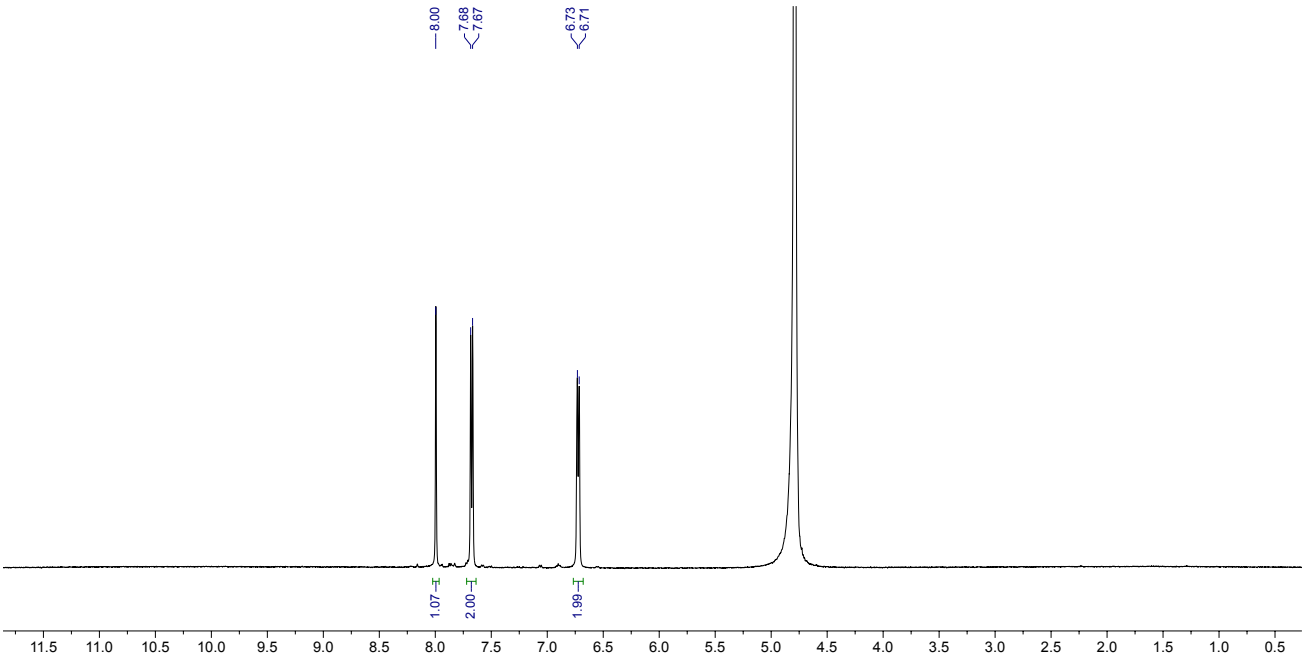

Fig. S1 ^{1}H NMR spectrum of purified **2** (500 MHz, D_2O, 298 K).

2. NMR characterization of $\mathbf{2}_2\subset\mathbf{1}$

Inclusion complex $\mathbf{2}_2\subset\mathbf{1}$ was obtained by mixing aqueous solutions of **1** and **2** in a 1:2 ratio.

^{1}H NMR (500 MHz, D_2O, 298 K): δ = 9.30 (s, 4H, $\mathbf{1}_\mathbf{a}$), 9.15 (s, 4H, $\mathbf{1}_\mathbf{d}$), 8.98 (s, 4H, $\mathbf{1}_{\mathbf{d}'}$), 7.95 (br, 4H, $\mathbf{2}_\beta$), 7.83 (s, $\mathbf{1}_\mathbf{b}$), 7.79 (s, $\mathbf{1}_\mathbf{c}$), 7.66 (s, $\mathbf{1}_\mathbf{h}$), 7.46 (s, $\mathbf{1}_\mathbf{g}$), 7.41 (br, $\mathbf{1}_\mathbf{e}$), 7.29 (br, $\mathbf{1}_\mathbf{f}$), 6.76 (s, 4H, $\mathbf{2}_\alpha$), 6.58 (d, J = 8.06 Hz, 4H, $\mathbf{2}_\gamma$), 3.21 (s, 8H, $\mathbf{1}_{\mathbf{j}\ ax}$), 3.09–3.01 (br, 16H, $\mathbf{1}_{\mathbf{j}\ eq}$), 2.89 (s, 12H, $\mathbf{1}_{\mathbf{i}\ ax}$), 2.86 (s, 12H, $\mathbf{1}_{\mathbf{i}\ ax}$), 2.74 (s, 12H, $\mathbf{1}_{\mathbf{i}\ eq}$), 2.65 (s, 12H, $\mathbf{1}_{\mathbf{i}\ eq}$), 2.61 (s, 12H, $\mathbf{1}_{\mathbf{i}\ eq}$), 2.58 (s, 12H, $\mathbf{1}_{\mathbf{i}\ eq}$).

^{13}C{^{1}H} NMR (125 MHz, D_2O, 298 K): δ = 185.0 ($2_{C=O}$), 151.1 ($\mathbf{2}_{C-SO_3}$), 138.6, 138.3 ($\mathbf{1}_\mathbf{a}$), 138.0 ($\mathbf{1}_\mathbf{d}$), 137.7 ($\mathbf{1}_{\mathbf{d}'}$), 137.0, 136.7, 134.0 ($\mathbf{2}_\beta$), 129.1 ($\mathbf{1}_\mathbf{b}$), 128.9 ($\mathbf{1}_\mathbf{f}$), 128.6 ($\mathbf{1}_\mathbf{e}$), 121.1 ($\mathbf{1}_\mathbf{c}$), 120.7 ($\mathbf{2}_\alpha$), 119.4, 113.1 ($\mathbf{1}_\mathbf{g}$), 112.7 ($\mathbf{2}_\gamma$), 111.6 ($\mathbf{1}_\mathbf{h}$), 62.6 ($\mathbf{1}_{\mathbf{j}\ ax}$), 62.5 ($\mathbf{1}_{\mathbf{j}\ eq}$), 50.5 ($\mathbf{1}_{\mathbf{i}\ eq}$), 50.4 ($\mathbf{1}_{\mathbf{i}\ ax}$), 50.4 ($\mathbf{1}_{\mathbf{i}\ eq}$), 50.2 ($\mathbf{1}_{\mathbf{i}\ ax}$), 50.0 ($\mathbf{1}_{\mathbf{i}\ eq}$), 49.6 ($\mathbf{1}_{\mathbf{i}\ eq}$).

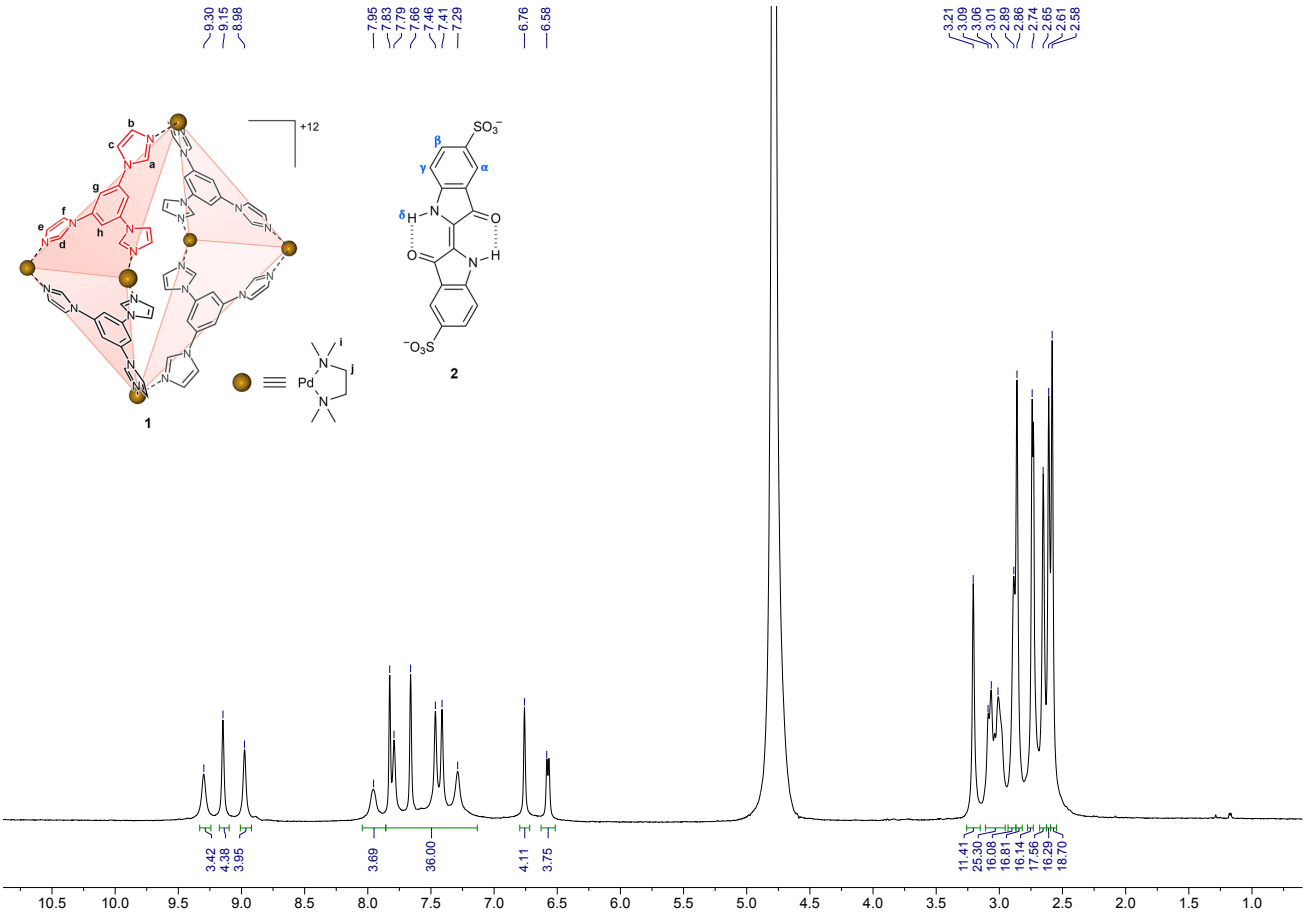

Fig. S2 ^{1}H NMR spectrum of $\mathbf{2}_2\subset\mathbf{1}$ (500 MHz, D_2O, 298 K). The peaks at 3.04 ppm and 2.73 ppm are due to residual free TMEDA (*N*,*N*,*N*′,*N*′-tetramethylethylenediamine; Pd's ancillary ligand).

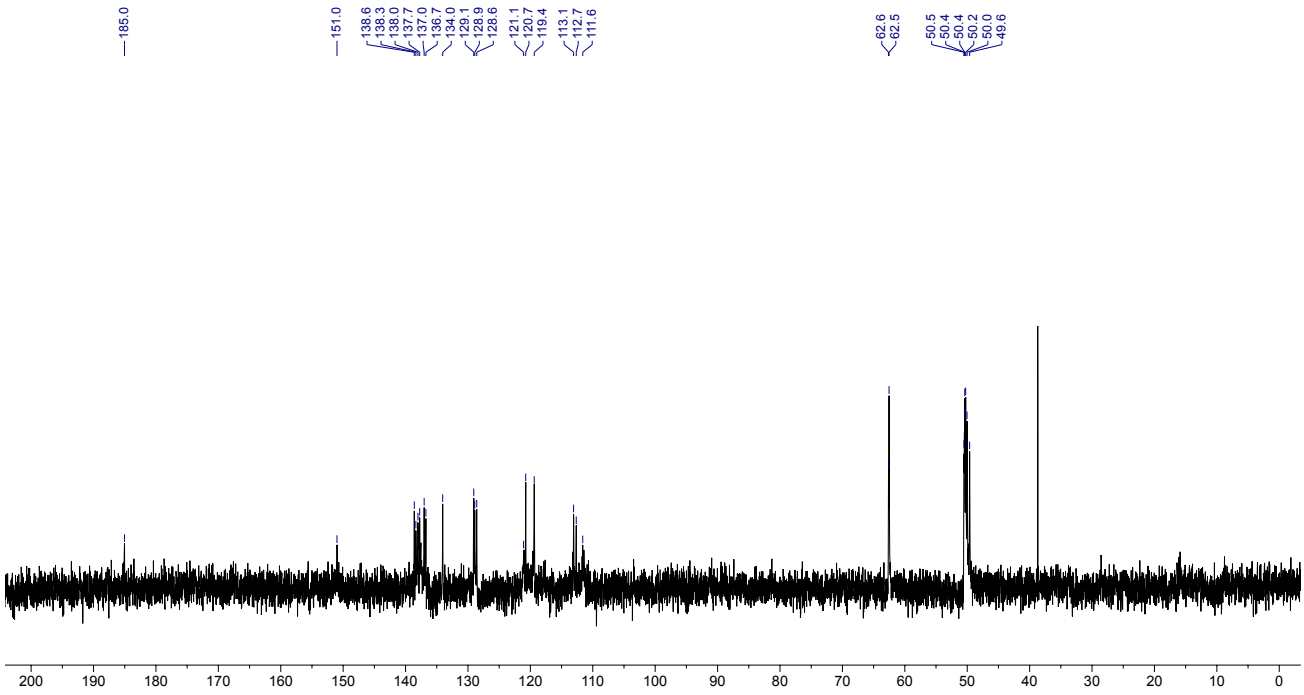

Fig. S3 $^{13}C\{^{1}H\}$ NMR spectrum of $\mathbf{2}_2\subset\mathbf{1}$ (125 MHz, D_2O, 298 K).

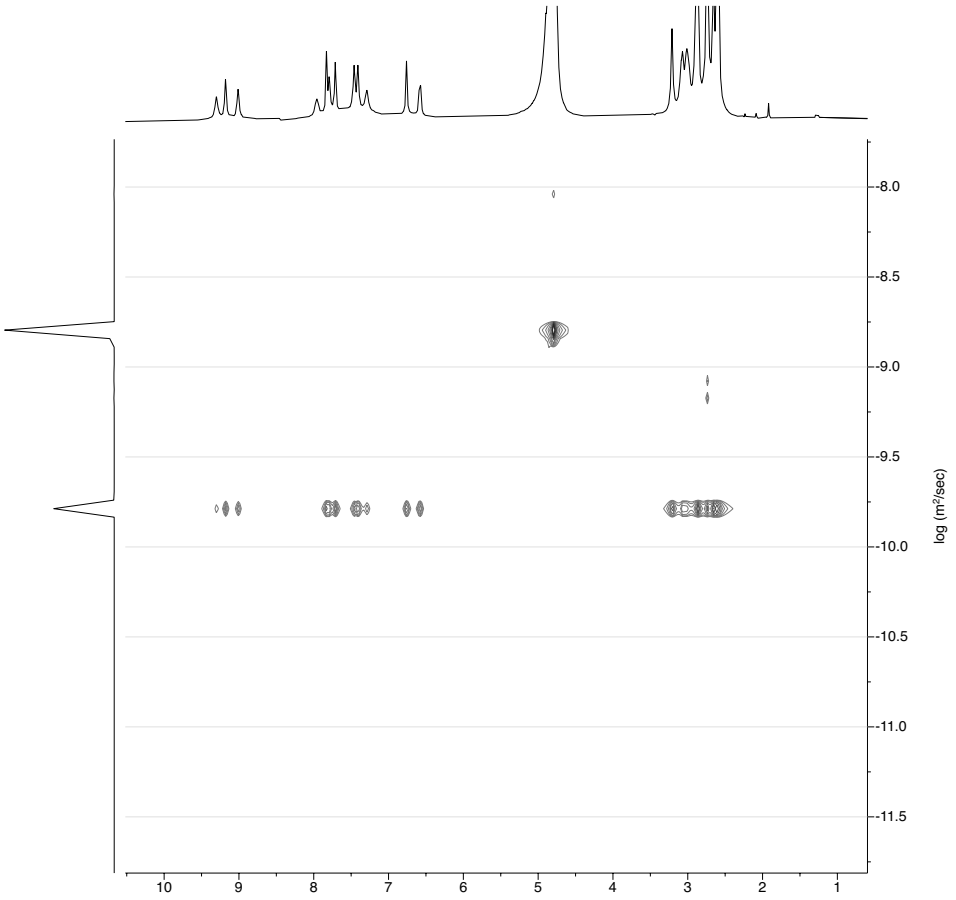

Fig. S4 ^{1}H DOSY NMR spectrum of $\mathbf{2}_2\subset\mathbf{1}$ (500 MHz, D_2O, 298 K).

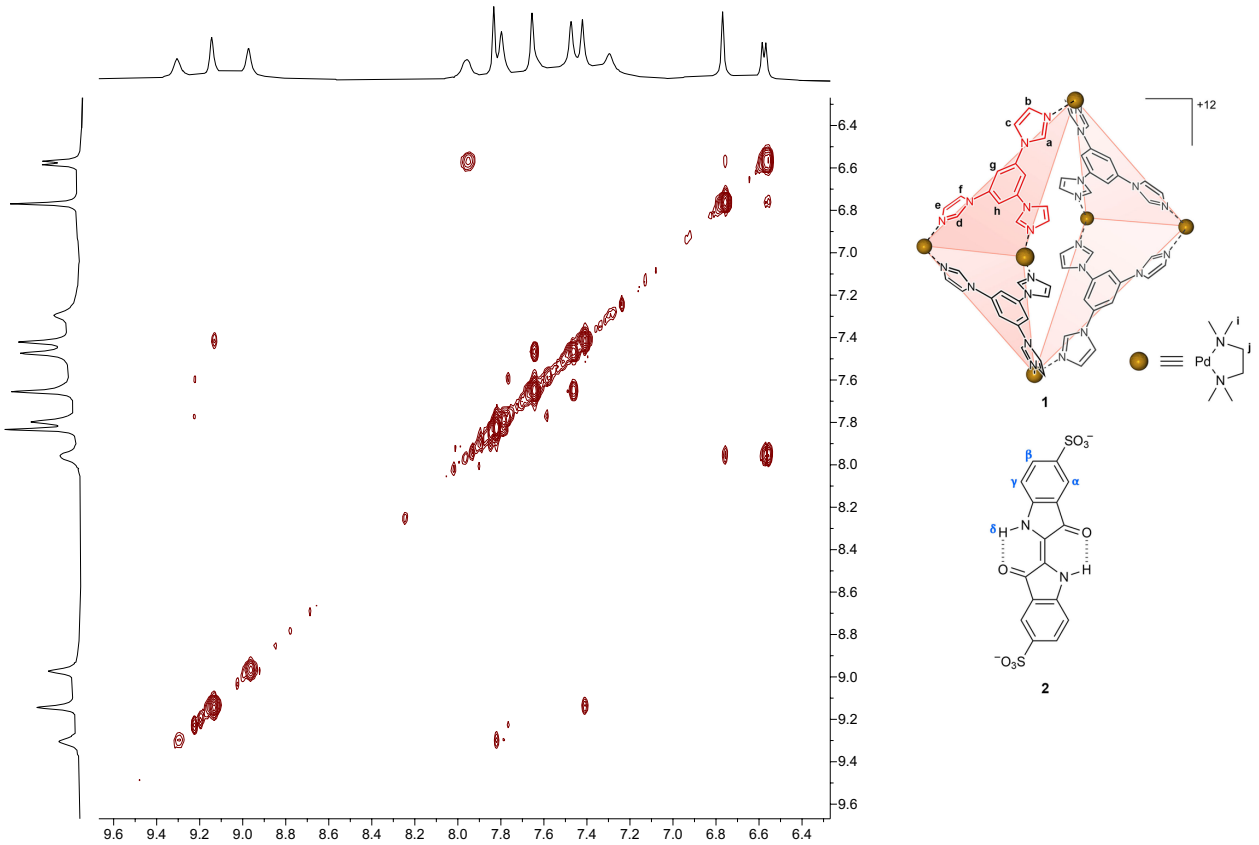

Fig. S5 Partial ^{1}H–^{1}H COSY NMR spectrum of $\mathbf{2}_2\subset\mathbf{1}$ (500 MHz, D_2O, 298 K). Notable correlations: $\mathbf{2}_{\alpha}$–$\mathbf{2}_{\beta}$, $\mathbf{2}_{\alpha}$–$\mathbf{2}_{\gamma}$, $\mathbf{2}_{\beta}$–$\mathbf{2}_{\gamma}$, $\mathbf{1}_{a}$–$\mathbf{1}_{b}$, $\mathbf{1}_{d}$–$\mathbf{1}_{f}$, $\mathbf{1}_{g}$–$\mathbf{1}_{h}$.

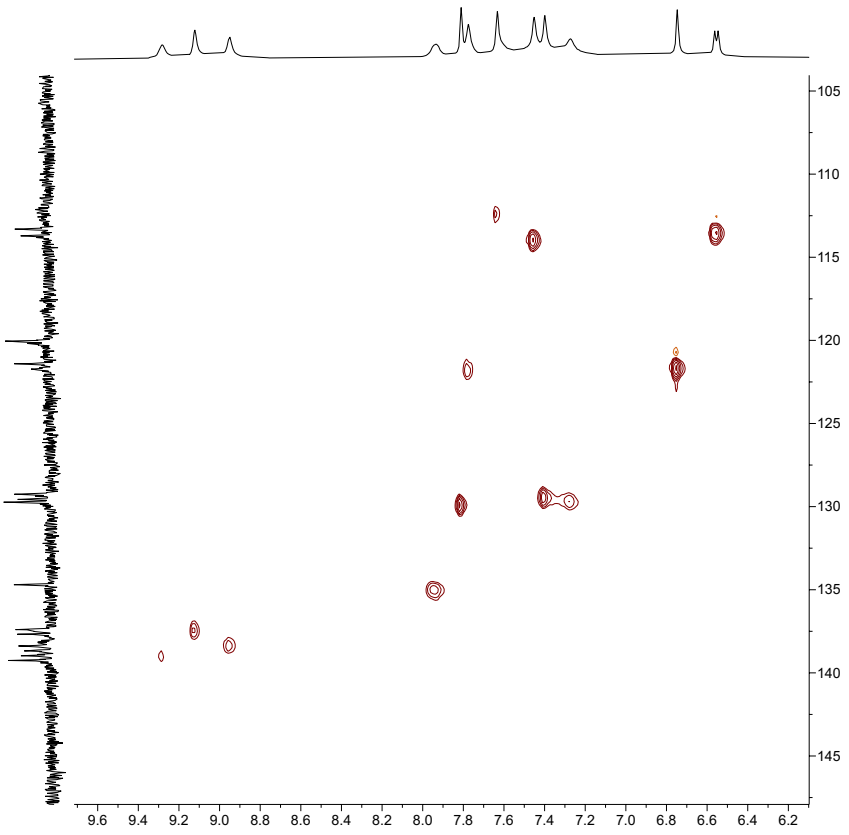

Fig. S6 Partial ^{1}H–^{13}C HSQC NMR spectrum of $\mathbf{2}_2\subset\mathbf{1}$ (500 MHz, D_2O, 298 K).

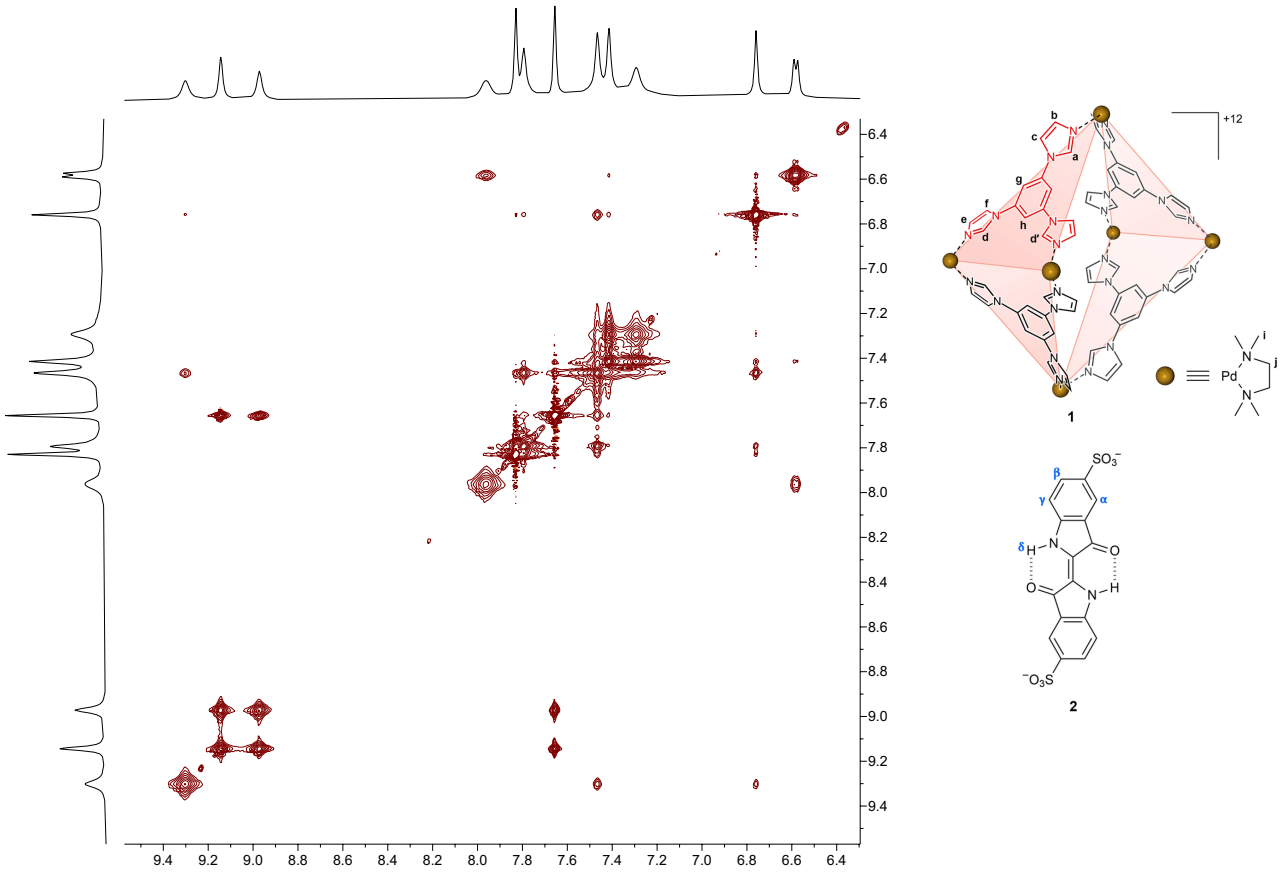

Fig. S7 Partial ^{1}H–^{1}H NOESY NMR spectrum of $\mathbf{2}_2\subset\mathbf{1}$, focusing on the aromatic region (500 MHz, D_2O, 298 K). Notable nOe correlations host–guest correlations: $\mathbf{2}_{\alpha}$–$\mathbf{1}_{a}$, $\mathbf{2}_{\alpha}$–$\mathbf{1}_{b}$, $\mathbf{2}_{\alpha}$–$\mathbf{1}_{c}$, $\mathbf{2}_{\alpha}$–$\mathbf{1}_{e}$, $\mathbf{2}_{\alpha}$–$\mathbf{1}_{f}$, $\mathbf{2}_{\alpha}$–$\mathbf{1}_{g}$, $\mathbf{2}_{\gamma}$–$\mathbf{1}_{e}$, $\mathbf{2}_{\gamma}$–$\mathbf{1}_{f}$, and $\mathbf{2}_{\gamma}$–$\mathbf{1}_{g}$. In addition, the spectrum shows many nOe correlations between different protons of cage **1**, which served to confirm the peak assignment; these include $\mathbf{1}_{a}$–$\mathbf{1}_{g}$, $\mathbf{1}_{b}$–$\mathbf{1}_{g}$, $\mathbf{1}_{c}$–$\mathbf{1}_{g}$, $\mathbf{1}_{d}$–$\mathbf{1}_{d'}$, $\mathbf{1}_{d}$–$\mathbf{1}_{h}$, $\mathbf{1}_{d'}$–$\mathbf{1}_{h}$, $\mathbf{1}_{e}$–$\mathbf{1}_{f}$, $\mathbf{1}_{f}$–$\mathbf{1}_{g}$, and $\mathbf{1}_{g}$–$\mathbf{1}_{h}$.

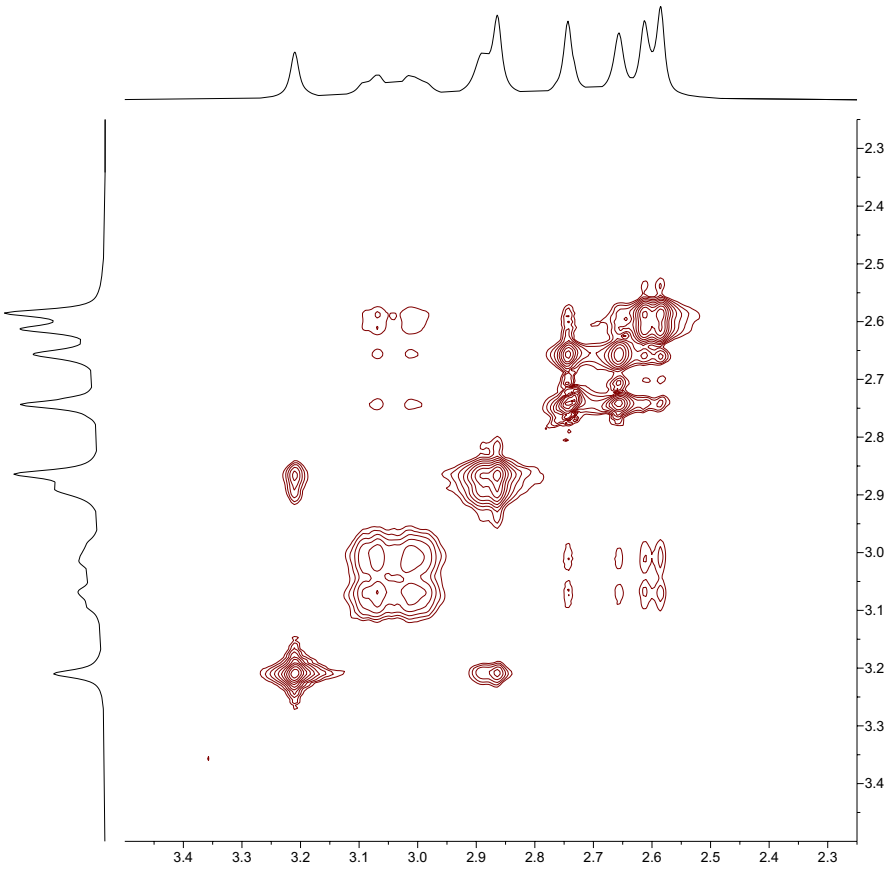

Fig. S8 Partial ^{1}H–^{1}H NOESY NMR spectrum of $\mathbf{2}_2\subset\mathbf{1}$, focusing on the aliphatic region (500 MHz, D_2O, 298 K).

3. NMR characterization of **2⊂1**

Inclusion complex **2⊂1** was obtained as a mixture with $\mathbf{2}_2\subset\mathbf{1}$ and **1** by treating **2** with an excess of **1**.

^{1}H NMR (500 MHz, D_2O, 298 K; guest peaks only): δ = 7.94 (br, 4H, $\mathbf{2}_{\beta'}$), 6.95 (br, 4H, $\mathbf{2}_{\gamma'}$), 6.91 (s, 4H, $\mathbf{2}_{\alpha'}$).

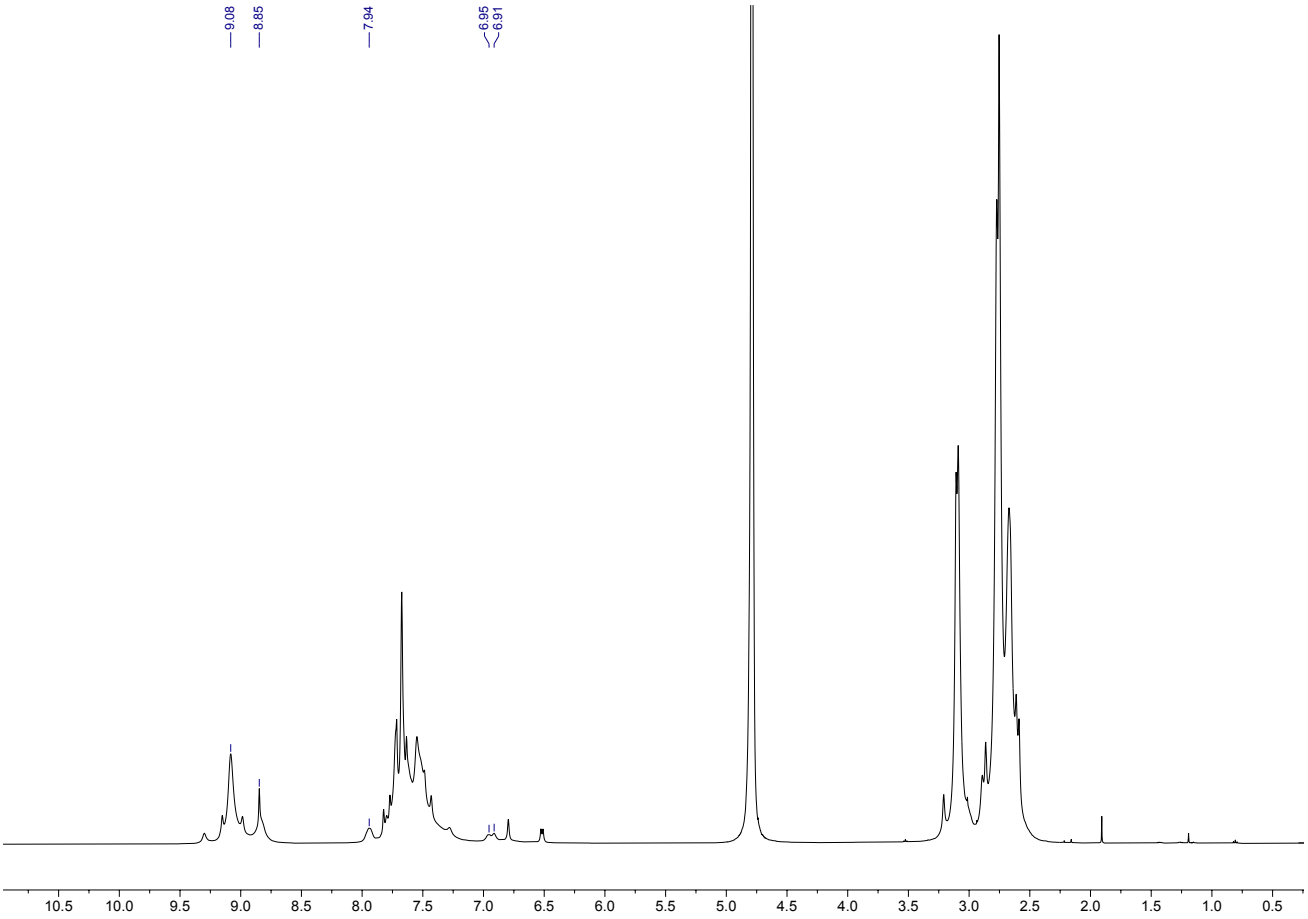

Fig. S9 ^{1}H NMR spectrum of a 2:1 mixture of **1** and **2** (500 MHz, D_2O, 298 K). Note that in addition to the three acidic imidazole proton signals due to $\mathbf{2}_2\subset\mathbf{1}$ (δ = 9.30, 9.15, and 8.99 ppm), only two large acidic imidazole proton signals are observed at chemical shifts expected from the free **1** (δ = 9.08 and 8.85 ppm); this result suggests that the acidic imidazole protons of **2⊂1** appear at chemical shifts very similar to those of free **1**.

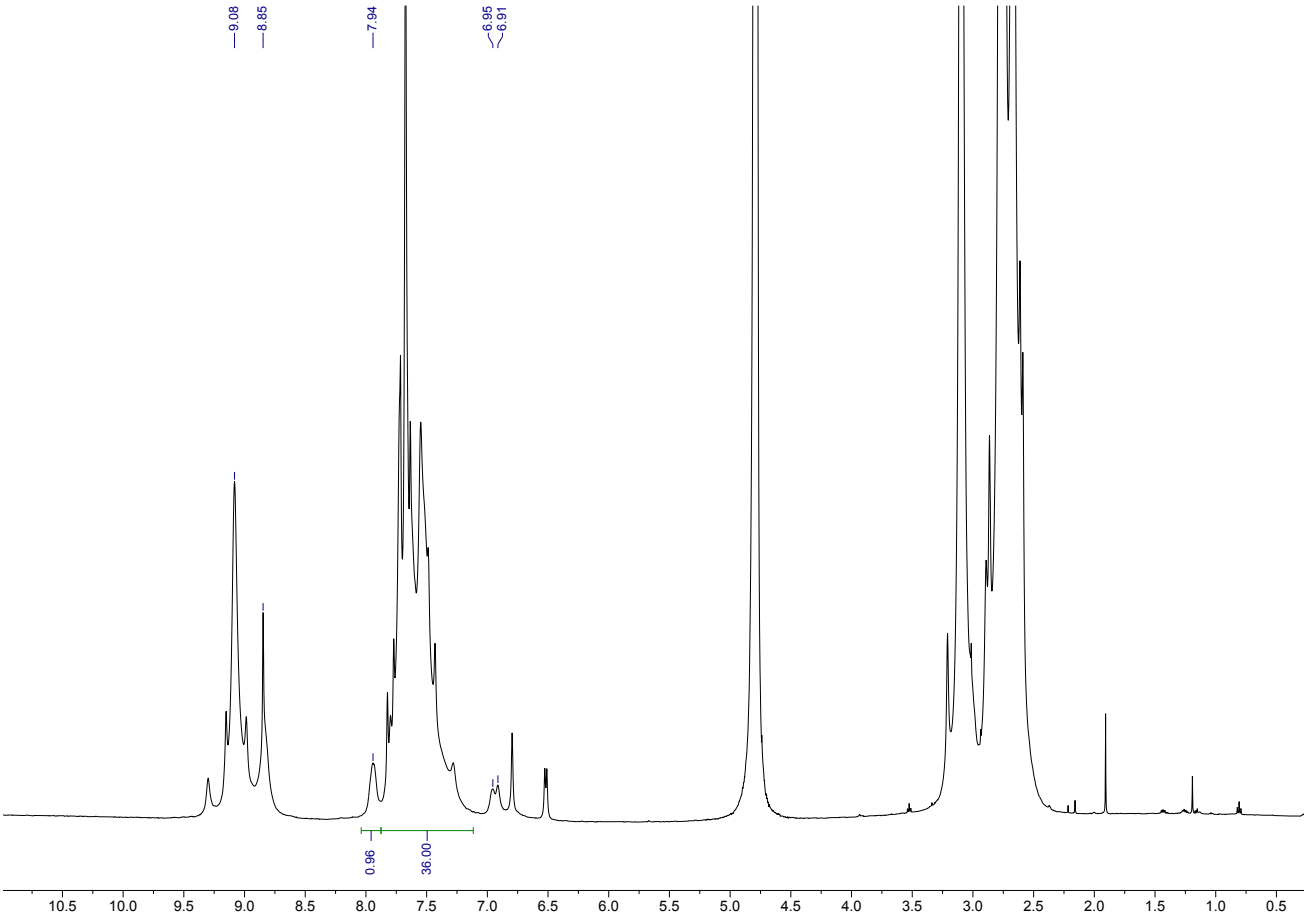

Fig. S10 ^{1}H NMR spectrum of a 2:1 mixture of **1** and **2** (500 MHz, D_2O, 298 K) (magnified view from Fig. S9).

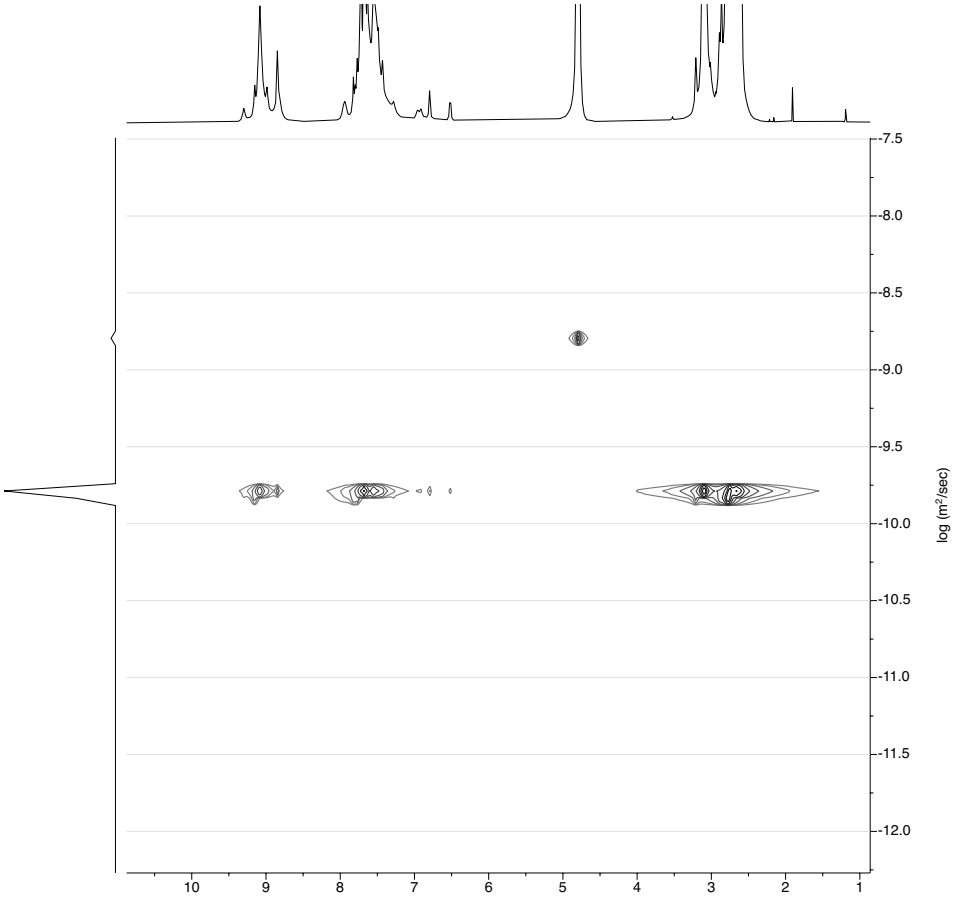

Fig. S11 ^{1}H DOSY NMR spectrum of a 2:1 mixture of **1** and **2** (500 MHz, D_2O, 298 K).

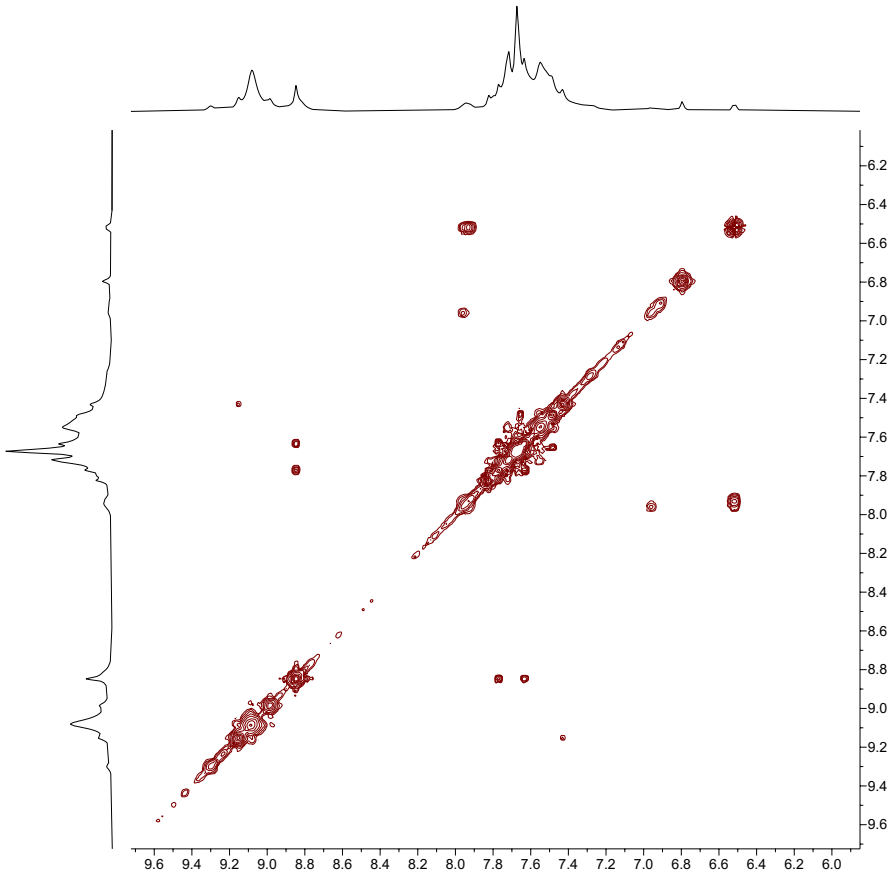

Fig. S12 Partial $^{1}H–^{1}H$ COSY NMR spectrum of a 2:1 mixture of **1** and **2** (500 MHz, D_2O, 298 K).

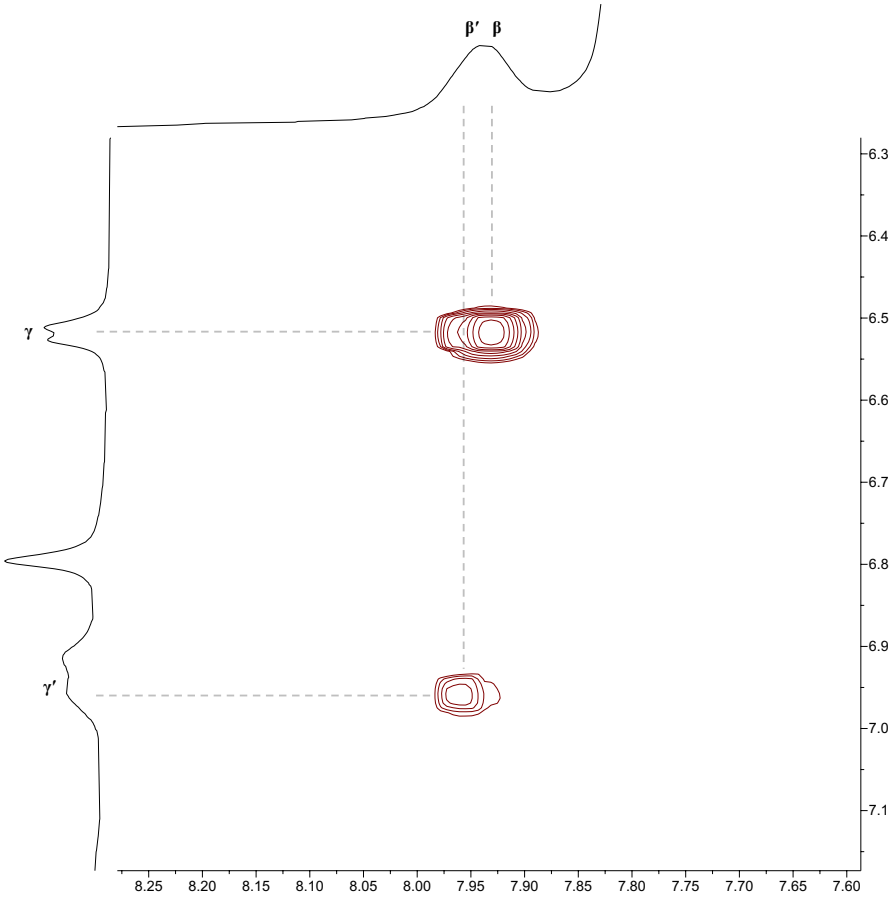

Fig. S13 Partial ^{1}H–^{1}H COSY NMR spectrum of a 2:1 mixture of **1** and **2** (500 MHz, D_2O, 298 K) (magnified view from Fig. S12).

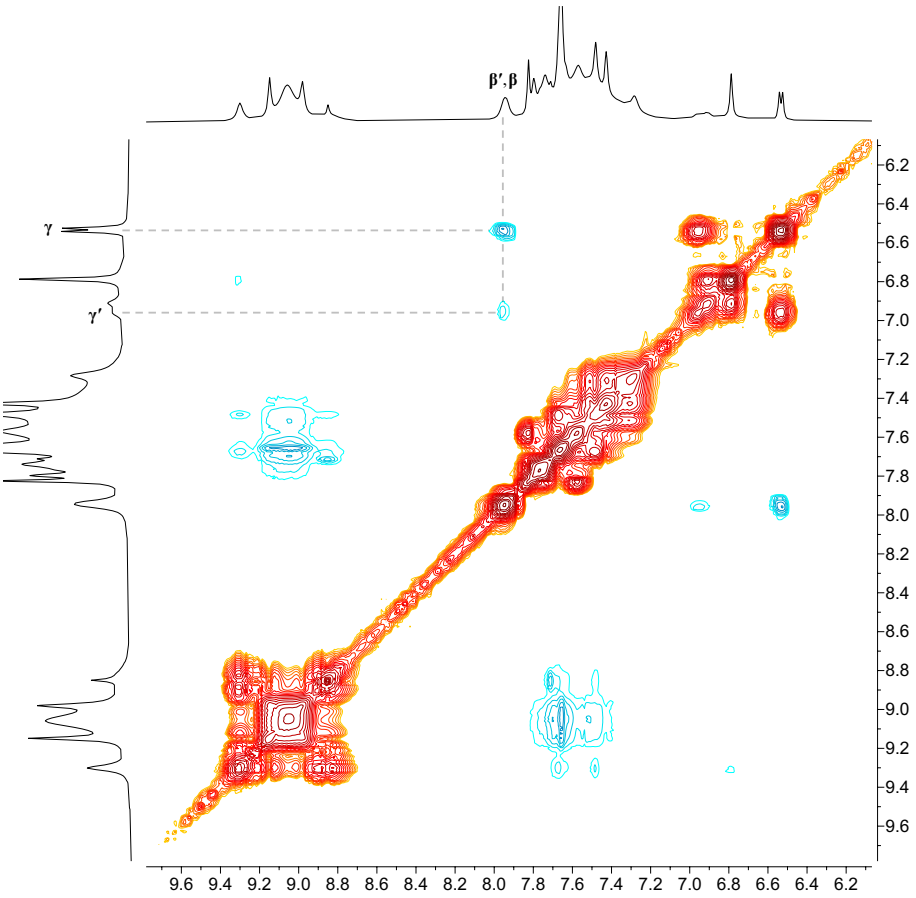

Fig. S14 Partial ^{1}H–^{1}H ROESY NMR spectrum of **1** and **2** mixed in a 2:1 ratio (500 MHz, D_2O, 298 K). The peak at 7.95 ppm (marked in the horizontal spectrum) correlates with both $\mathbf{2}_{\gamma}$ and $\mathbf{2}_{\gamma'}$ (denoted in the vertical spectrum), indicating that is due to **2**'s **β** proton in both 1:1 and 2:1 inclusion complexes (i.e., $\mathbf{2}_{\beta}$ and $\mathbf{2}_{\beta'}$).

4. NMR titrations

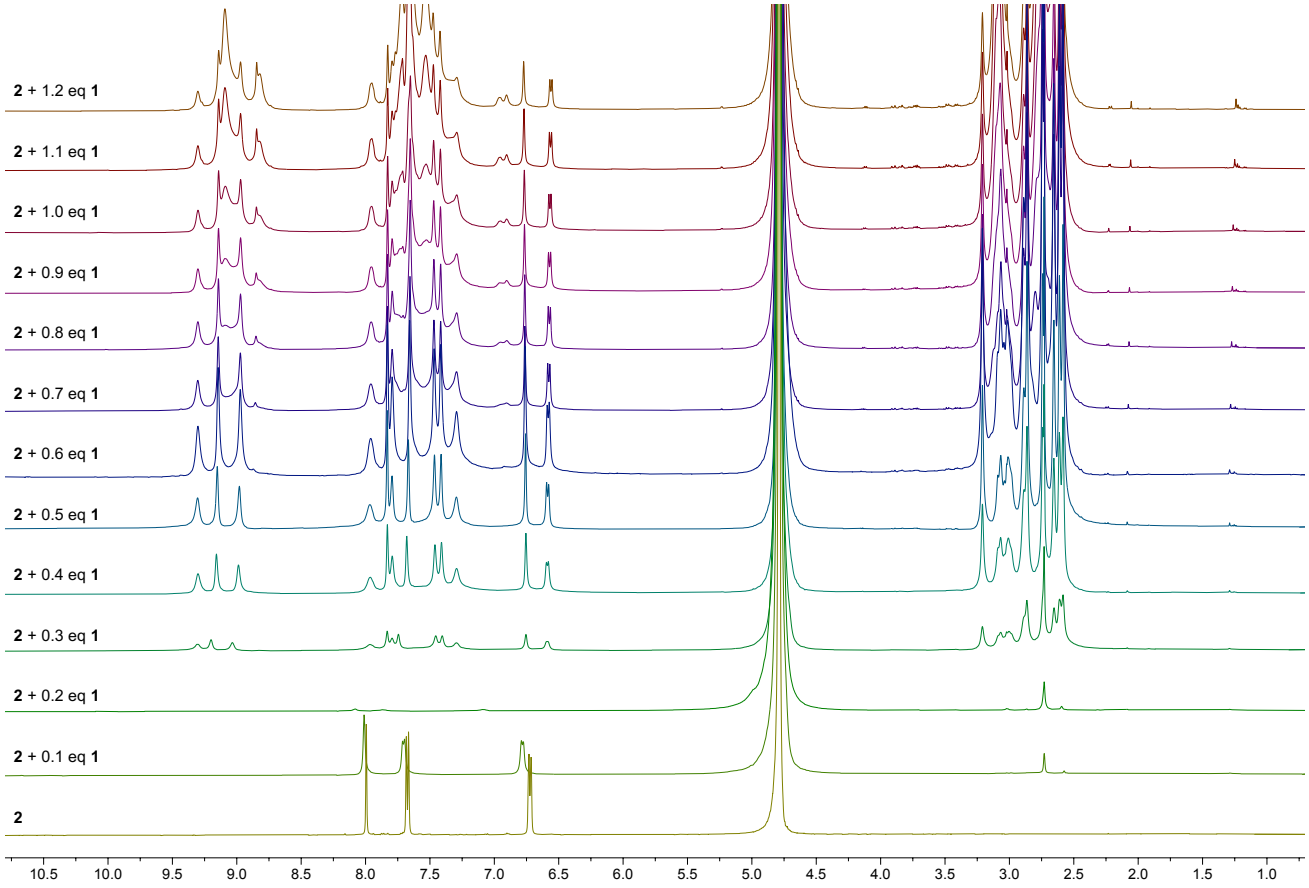

Fig. S15 A series of full-range ^{1}H NMR spectra obtained during titration of **2** (bottom spectrum) with **1** (up to 1.2 eq; 500 MHz, D_2O, 298 K).

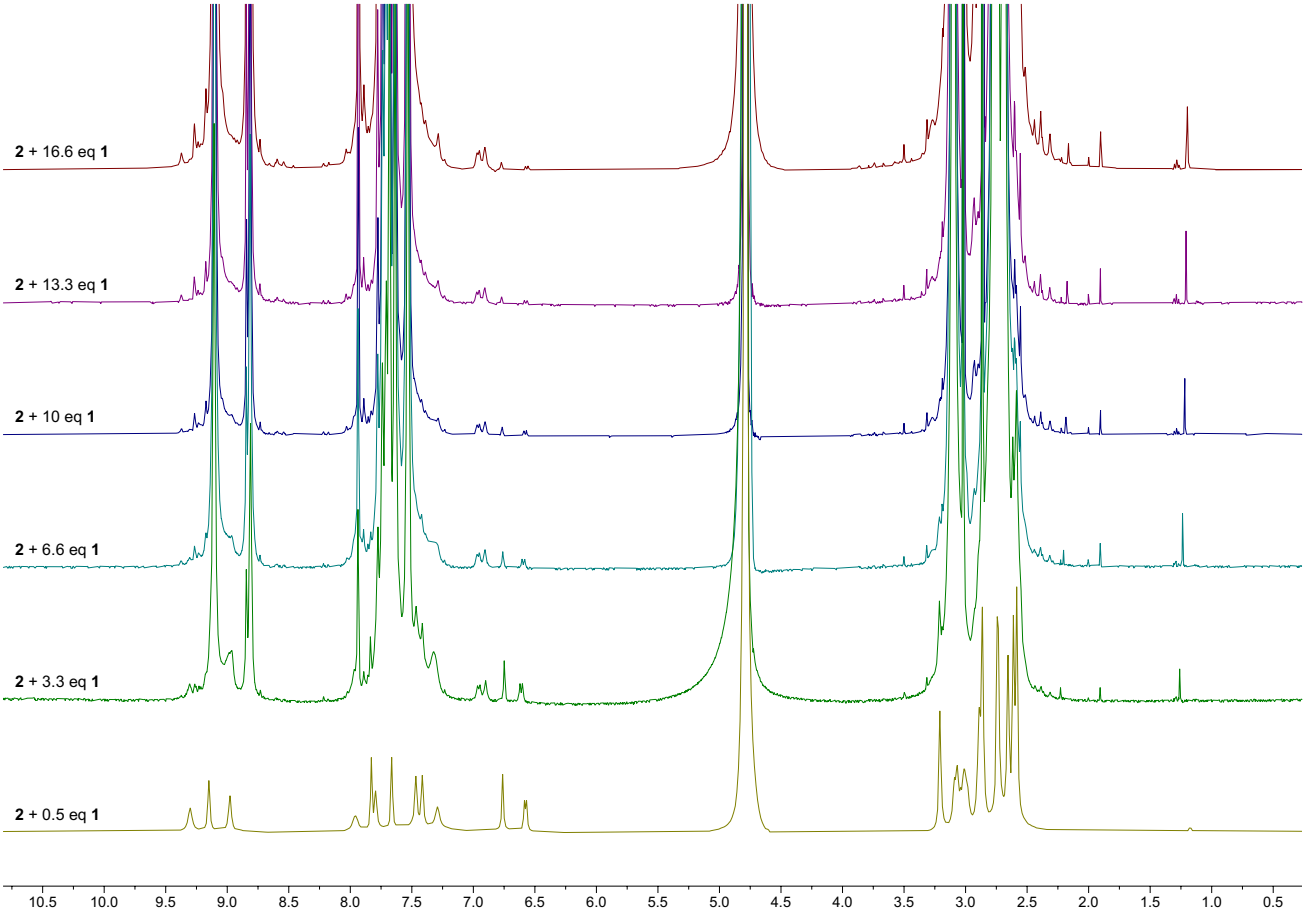

Fig. S16 A series of full-range ^{1}H NMR spectra obtained during titration of **2** with **1** (up to 16.6 eq; 400 MHz, D_2O, 298 K; bottom spectrum: 500 MHz, D_2O, 298 K).

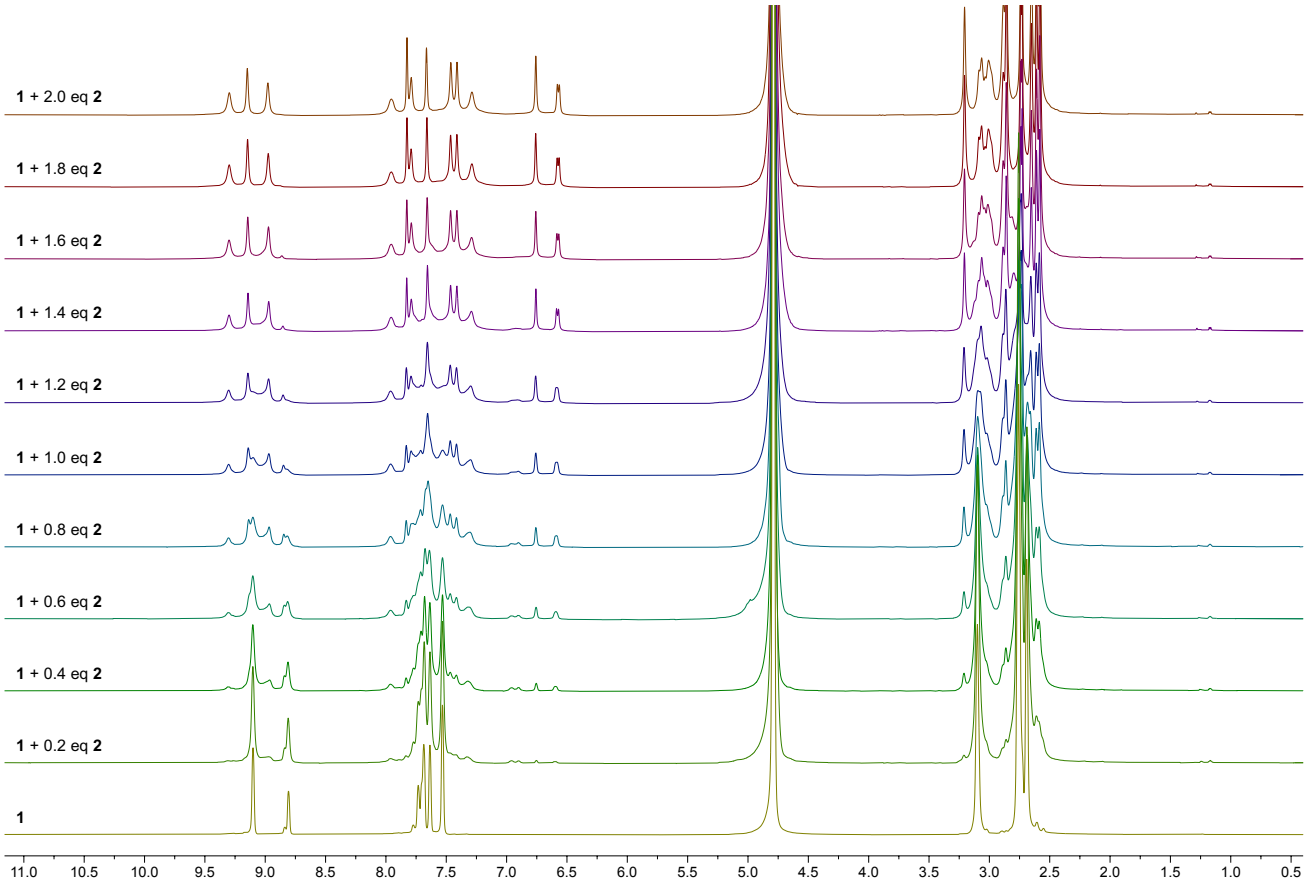

Fig. S17 A series of full-range ^{1}H NMR spectra obtained during titration of **1** (bottom spectrum) with **2** (500 MHz, D_2O, 298 K).

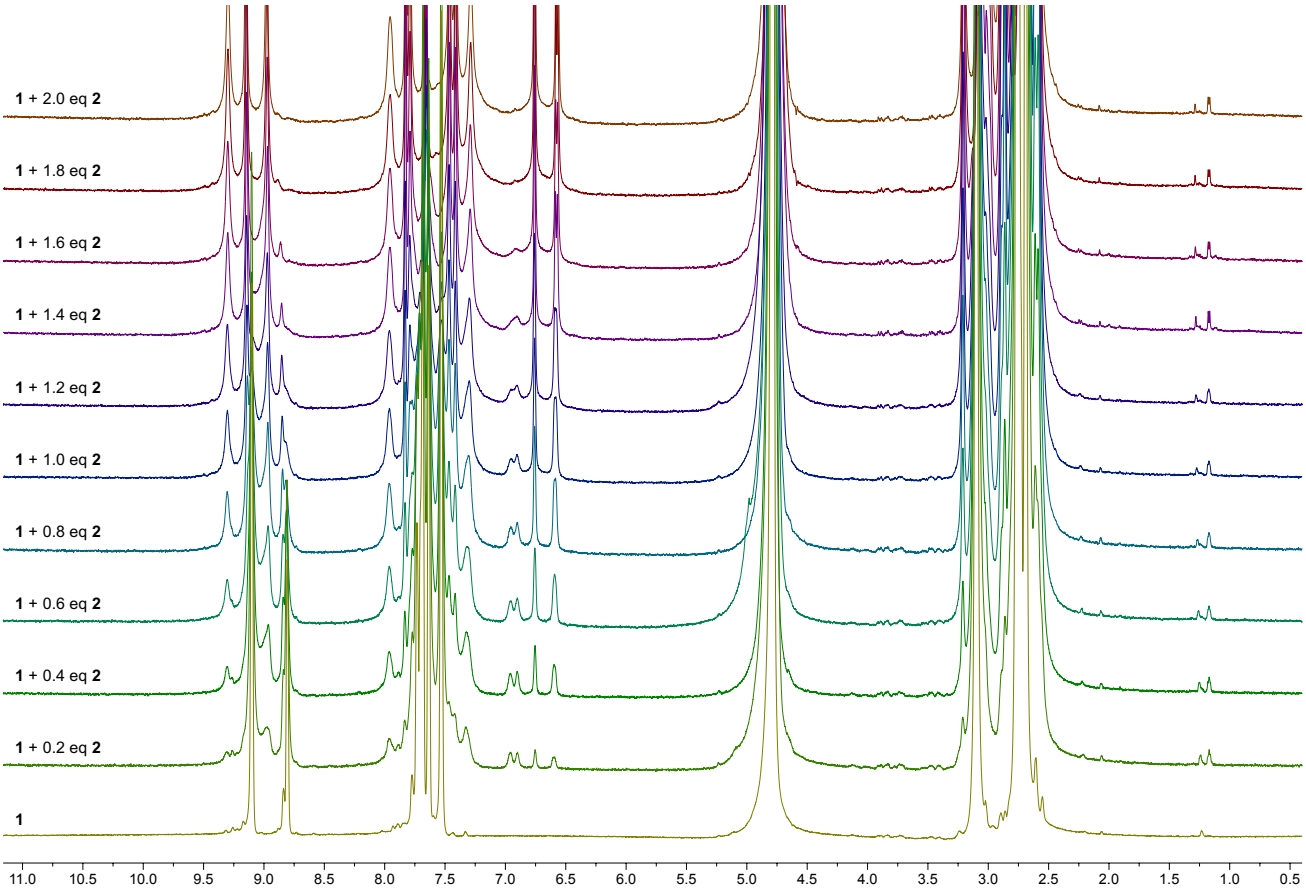

Fig. S18 A series of full-range ^{1}H NMR spectra obtained during titration of **1** (bottom spectrum) with **2** (magnified view from Fig. S17) (500 MHz, D_2O, 298 K).

5. X-ray data collection and structure refinement

Single crystals of the inclusion complex $\mathbf{2}_2\subset\mathbf{1}$ were obtained by two different ways: by slow water evaporation, and by acetone vapor diffusion. In the both cases, the crystal was coated in Paratone oil (Hampton Research), mounted on a MiTeGen loop, and flash-frozen in the liquid nitrogen stream of the Oxford Cryostream. Data collection was performed under a stream of nitrogen at 100 K. The diffraction data of the crystal obtained by water evaporation were collected on a Rigaku Synergy diffractometer using Mo-Kα radiation (0.7107 Å) and a Dectris Pilatus 3R 300K CdTe detector. The diffraction data of the crystal obtained by acetone vapor diffusion were collected on a Rigaku XtaLAB Synergy R Rotating anode system diffractometer using Cu-Kα radiation (1.54184 Å) and a HyPix-Arc 150 detector.

The data were collected, processed, and reduced with the CrysAlis^{PRO} software package (Rigaku Oxford Diffraction, CrysAlisPro Software system 1.171.40, Rigaku Corporation, 2018). The structures were solved by direct methods using SHELXT[1] as implemented in the Olex2 software GUI.[2] The structures were refined by full-matrix least-squares methods on *F*2 with SHELXL. All non-hydrogen atoms were further refined by SHELXL with anisotropic displacement coefficients. Hydrogen atoms were placed in calculated positions,

[1] G. M. Sheldrick, *Acta Cryst. A* 2008, **64**, 112.
[2] O. V. Dolomanov, L. J. Bourhis, R. J. Gildea, J. A. K. Howard and H. Puschmann, *J. Appl. Cryst.* 2009, **42**, 339.

assigned isotropic displacement coefficients, U(H) = 1.2U(C) or 1.5U (C-methyl), and their coordinates were allowed to ride on their respective carbons. Ordered counterions and water oxygens were placed in the electron density peaks where possible. Some of these molecules were refined with half-occupancy. The water hydrogen atoms were not seen. Squeeze protocol of PLATON was used.[3] Crystallographic data and refinement parameters are summarized in Table S1 below.

	Prepared by water evaporation	Prepared by acetone diffusion
CCDC	2126310	2128952
Formula	$C_{256}H_{320}N_{98}Na_2O_{181}Pd_{12}S_8$	$C_{256}H_{320}N_{88}O_{93}Pd_{12}S_8$
Formula weight*	9245.38	7651.26
Crystal system	Triclinic	Triclinic
Space group	$P\bar{1}$	$P\bar{1}$
Crystal size (mm)	0.29×0.28×0.10	0.12×0.12×0.20
Crystal color and shape	Dark blue plate	Blue plate
Temperature (K)	100	100
Wavelength (Å)	0.71073	1.5184
a (Å)	18.9000(5)	18.5972(2)
b (Å)	20.5889(5)	20.7368(3)
c (Å)	30.2601(8)	30.3057(3)
α (º)	78.576(2)	78.306(1)
β (º)	82.416(2)	82.382(1)
γ (º)	82.952(2)	82.000(1)
Volume (Å^3)	11384.3(5)	11267.5(2)
Z	1	1
ρ_{calcd} (g·cm^{-1})	1.349	1.128
μ (mm^{-1})	0.595	4.694
No. of reflections (unique)	216791 (49948)	296248 (45350)
R_{int}	0.0656	0.0488
Completeness to θ (%)	99.4	99.2
Data / restraints / parameters	49948 / 23 / 2545	45350 / 117 / 2216
Goodness-of-fit on F^2	1.058	1.085
Final R_1 and wR_2 indices [$I>2\sigma(I)$]	0.1018, 0.2666	0.0659, 0.1845
R_1 and wR_2 indices (all data)	0.1327, 0.2666	0.0732, 0.1917

Table S1 Crystallographic data and refinement parameters for **2_2⊂1** crystallized in two different ways. (*Derived from the crystal structure)

[3] A. L. Spek, *Acta Cryst.* C 2015, **71**, 9.

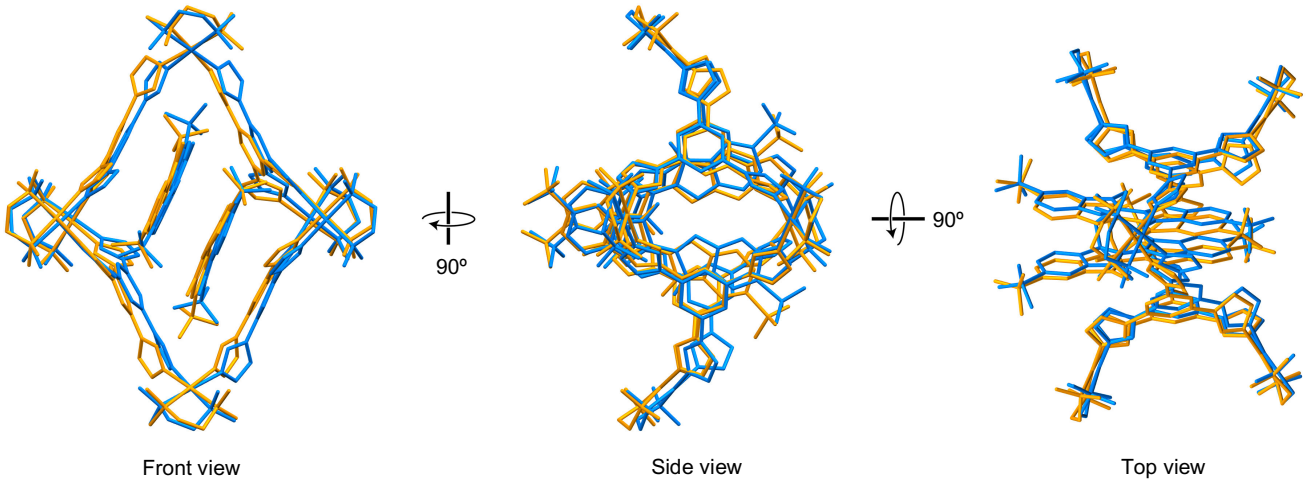

Fig. S19 Comparison of the solid-state structures of $\mathbf{2}_2\subset\mathbf{1}$ crystallized by water evaporation (orange) and acetone vapor diffusion (blue). Hydrogens, small ions, and water molecules were omitted for clarity.

6. Isothermal calorimetry titrations

Stock solutions of **1** (468 μM) and **2** (47.4 μM) in double-distilled water were prepared (the solution of **1** was allowed to equilibrate for one day). The syringe was charged with 100 μL of the stock solution of **1** and the cell was charged with 310 μL of the stock solution of **2**. Eighteen aliquots of the stock solution of **1** were injected; the first aliquot was 0.4 μL; the remaining 17 were 1 μL each. Each injection was carried out over 4 s, with a 150 s interval between two adjacent injections. The stirring rate was 750 rpm, the feedback was set to high, and the reference power was 10 μW. The blank (stock solution of **1** added to pure water) was also recorded and then subtracted from the titration data with the point-to-point tool. Data analysis was performed using MicroCal PEAQ-ITC Analysis Software; the Two Sets of Sites model was used to estimate the binding constants. The results are shown in Fig. S20 and Table S2.

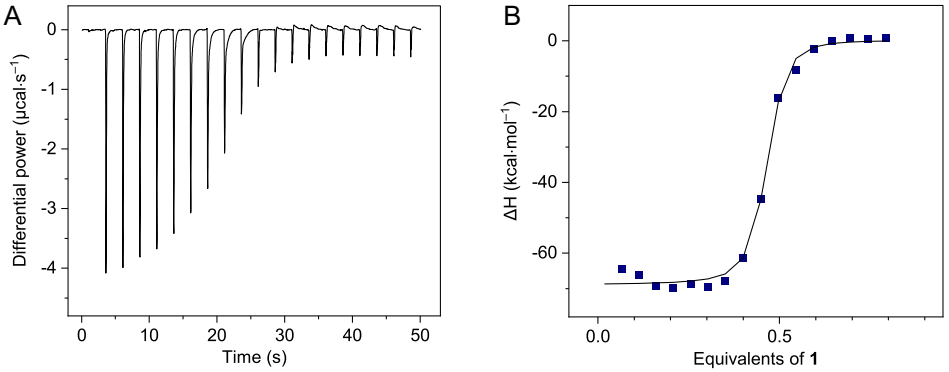

Fig. S20 (A) Plot of differential power vs. time for the titration of **2** (0.44 mM) with cage **1** (2.34 mM). (B) Plot of ΔH vs. the amount of **1** added fitted (line) to a 2:1 binding model.

Reaction	K_a (M^{-1})	ΔH (kJ·mol^{-1})	$-T\Delta S$ (kJ·mol^{-1})	ΔG (kJ·mol^{-1})
2 + **1** → **2**⊂**1**	2.78(±0.60)·10^6	–30.20(±0.75)	–7.00(±0.97)	–37.20(±0.26)
2⊂**1** + **1** → **2**$_2$⊂**1**	7.41(±0.82)·10^6	–30.20(±0.48)	–9.33(±0.51)	–39.55(±0.10)

Table S2 Thermodynamic and interaction parameters of the complexation of **2** with **1**.

7. UV–vis titrations

*Titration of **2** with cage **1**:* Titration experiments were conducted in double-distilled water. Cage **1** (15 mg) was dissolved in water (0.5 mL) and the solution was allowed to equilibrate for one day. **2** (10 mg) was dissolved in 2 mL of water; 4 μL of the resulting solution was diluted with 1 mL of water and titrated with small aliquots of **1**, with a titration step of 0.23 μL (0.05 eq of cage). The injection rate was 2 min per aliquot; a UV–Vis absorption spectrum was recorded after each injection. The resulting spectra are shown in Fig. 4A (main text).

*Titration of **2** with an excess of cage **1**:* Titration experiments were conducted in double-distilled water. Cage **1** (30 mg) was dissolved in water (1.0 mL) and the solution was allowed to equilibrate for one day. **2** (2 mg) was dissolved in 0.5 mL of water; 10 μL of the resulting solution was diluted with 1 mL of water and titrated with small aliquots of **1** until 514 μL of the cage solution (56.4 eq of **1**) were added. The injection rate was 2 min per aliquot; a UV–Vis absorption spectrum was recorded after each injection. The resulting spectra are shown in Fig. 4C (main text).

*Titration of **1** with **2**:* Titration experiments were conducted in double-distilled water. **2** (2 mg) was dissolved in 0.5 mL of water. Cage **1** (15 mg) was dissolved in water (0.5 mL) and the solution was allowed to equilibrate for one day; 9.11 μL of the resulting solution was diluted with 1 mL of water and titrated with small aliquots of **2** until 36 μL of the solution of **2** (3.6 eq of **2**) were added. The injection rate was 2 min per aliquot; a UV–vis absorption spectrum was recorded after each injection. The resulting spectra are shown in Fig. S21A.

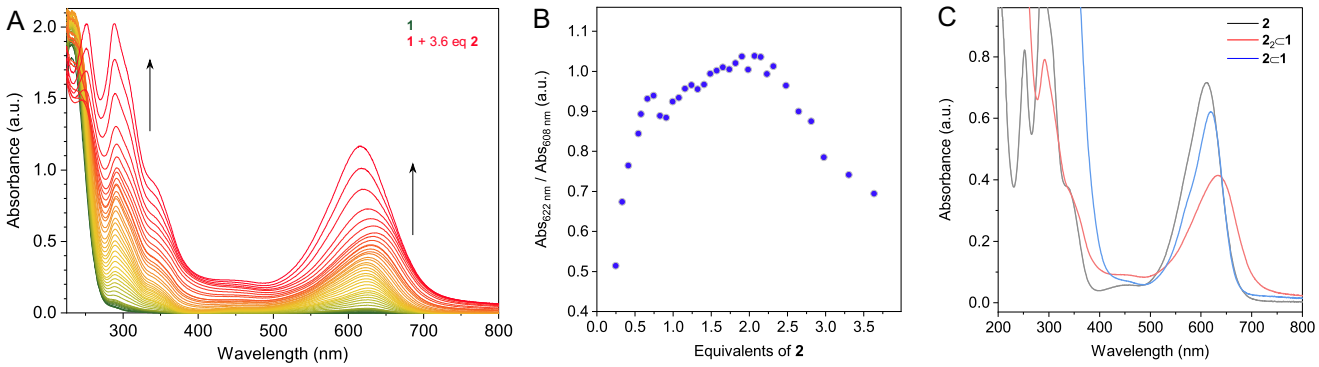

Fig. S21 (A) Evolution of UV–Vis absorption spectra upon the gradual addition of **2** to a solution of **1**. Note that with increasing **2**, the wavelength of maximum absorption in the 600–650 nm range moves to the right and then moves back to the left. (B) Analysis of the data shown in the spectra. The *y*-axis was set as the ratio of the absorbance at 622 nm ($Abs_{622\,nm}$) to the absorbance at 608 nm ($Abs_{608\,nm}$); this ratio is high for a large fraction of $\mathbf{2}_2\subset\mathbf{1}$ but low for a large fraction of either $\mathbf{2}\subset\mathbf{1}$ and **2** (see the spectra in panel C). Initially, the absorption in the visible region originates from $\mathbf{2}\subset\mathbf{1}$ (**1** in the presence of a large excess of **2**); thus, $Abs_{622\,nm}$ / $Abs_{608\,nm}$ is low. At 2.0 eq of **2**, $Abs_{622\,nm}$ / $Abs_{608\,nm}$ reaches the highest value since all **2** is encapsulated as $\mathbf{2}_2\subset\mathbf{1}$. For >2 eq of **2**, all the cages are saturated; the mixture consists of $\mathbf{2}_2\subset\mathbf{1}$ and an increasing amount of **2**; thus, $Abs_{622\,nm}$ / $Abs_{608\,nm}$ gradually decreases. (C) UV–Vis absorption spectra of **2**, $\mathbf{2}_2\subset\mathbf{1}$, and **2** in the presence of 56.4 eq of **1** (denoted $\mathbf{2}\subset\mathbf{1}$), all at the same concentration of **2**. All the spectra shown in this figure are corrected for dilution.

8. Fluorescence titrations

*Titration of **2** with cage **1**:* Titration experiments were conducted in double-distilled water. Cage **1** (30 mg) was dissolved in water (1.0 mL) and the solution was allowed to equilibrate for one day. **2** (10 mg) was dissolved in 2.0 mL of water; 10.5 µL of the resulting solution was diluted with 1.0 mL of water and titrated with small aliquots of **1**, with a titration step of 1.0 µL (0.08 eq of **1**). The injection rate was 2 min per aliquot; a fluorescence spectrum was recorded after each injection (λ_{exc} = 600 nm). The resulting spectra are shown in Fig. S22A.

*Titration of **2** with an excess of cage **1**:* Titration experiments were conducted in double-distilled water. Cage **1** (15 mg) was dissolved in water (0.5 mL) and the solution was allowed to equilibrate for one day. **2** (10 mg) was dissolved in 2.0 mL of water; 2.7 µL of the resulting solution was diluted with 1.0 mL of water and titrated with small aliquots of **1** until 188 µL of the cage solution (~61 eq of **1**) were added. The injection rate was 2 min per aliquot; a fluorescence spectrum was recorded after each injection (λ_{exc} = 600 nm). The resulting spectra are shown in Fig. S22B.

*Titration of **1** with **2**:* Titration experiments were conducted in double-distilled water. **2** (10 mg) was dissolved in 2.0 mL of water. Cage **1** (30 mg) was dissolved in water (1.0 mL) and the solution was allowed to equilibrate for one day; 6.0 µL of the resulting solution was diluted with 1.0 mL of water and titrated with small aliquots of **2**, with a titration step of 1.0 µL (0.19 eq of **2**). The injection rate was 2 min per aliquot; a fluorescence spectrum was recorded after each injection (λ_{exc} = 600 nm). The resulting spectra are shown in Fig. S22C.

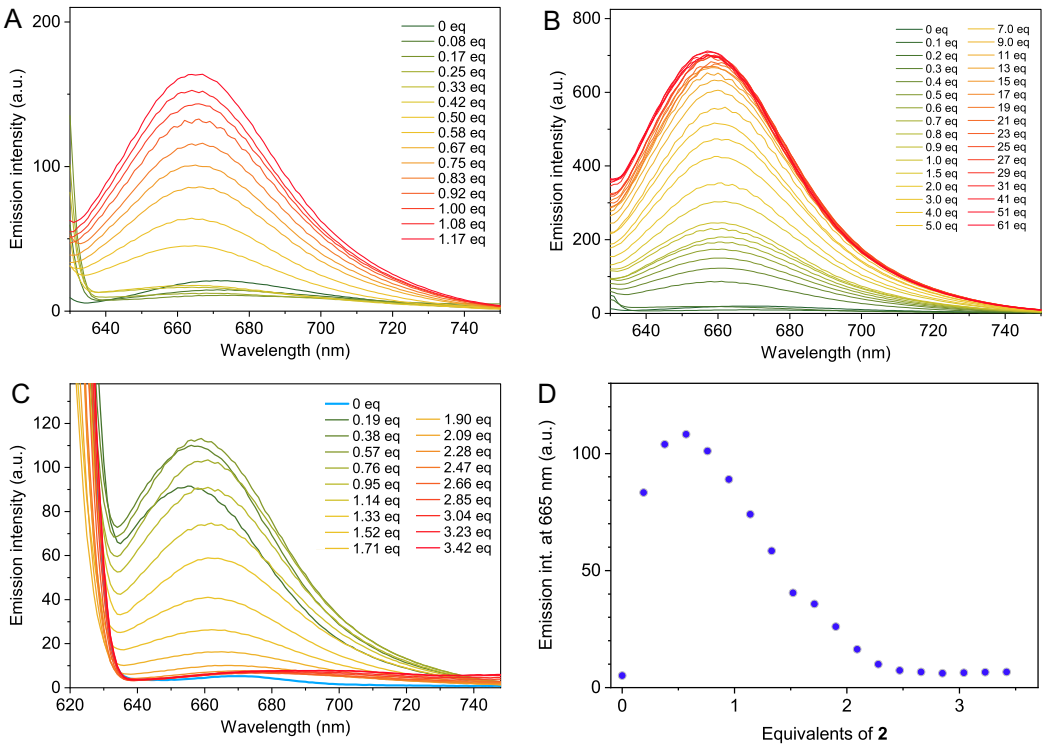

Fig. S22 (A) Evolution of fluorescence spectra upon the gradual addition of **1** (up to 1.17 eq) to a solution of **2**. (B) Evolution of fluorescence spectra upon the gradual addition of **1** (up to 61 eq) to a solution of **2**. (C) Evolution of fluorescence spectra upon the gradual addition of **2** to a solution of **1**. (D) Rapid increase followed by a slow decrease of emission observed during titration of **1** with **2**. All the spectra shown in this figure are corrected for dilution.